



COPY RIGHT



ELSEVIER
SSRN

2023 IJEMR. Personal use of this material is permitted. Permission from IJEMR must be obtained for all other uses, in any current or future media, including reprinting/republishing this material for advertising or promotional purposes, creating new collective works, for resale or redistribution to servers or lists, or reuse of any copyrighted component of this work in other works. No Reprint should be done to this paper, all copy right is authenticated to Paper Authors

IJEMR Transactions, online available on 05th Apr 2023. Link

[:http://www.ijiemr.org/downloads.php?vol=Volume-12&issue=Issue 04](http://www.ijiemr.org/downloads.php?vol=Volume-12&issue=Issue 04)

10.48047/IJEMR/V12/ISSUE 04/141

Title RELIABILITY ENHANCEMENT OF ISLANDED MICROGRID NETWORKS THROUGH HEURISTIC OPTIMIZATION-BASED DG SIZING AND PLACEMENT

Volume 12, ISSUE 04, Pages: 1098-1113

Paper Authors

Sireesha R, C. Srinivasa Rao, M. Vijay Kumar



USE THIS BARCODE TO ACCESS YOUR ONLINE PAPER

To Secure Your Paper As Per **UGC Guidelines** We Are Providing A Electronic Bar Code

RELIABILITY ENHANCEMENT OF ISLANDED MICROGRID NETWORKS THROUGH HEURISTIC OPTIMIZATION-BASED DG SIZING AND PLACEMENT

Sireesha R¹, C. Srinivasa Rao², M. Vijay Kumar³

¹ Research Scholar, EEE Department, JNTUA, Ananthapuramu. sireesha253@gmail.com

² Principal, G Pullaiah College of Engineering and Technology, Kurnool.

³ Professor, EEE Department, JNTUA, Ananthapuramu.

Abstract: Any disruption to a power distribution network affects the economy and daily lives. This study aims to transform conventional power distribution systems into autonomous microgrid networks by sizing and placing distributed generators optimally (DGs). First, N main DGs are placed to create an autonomous microgrid. Second, all possible combinations of initially deployed DGs are made, then 1 to $N-1$ DG outages are considered. The network's resiliency is analyzed by removing DGs one by one. This step analyzes load shedding, network power loss, and voltage limits. Based on the resiliency analysis, additional DGs are added to the transformed network. First and second step DG sizing and siting use heuristic methods (particle swarm optimisation and genetic algorithm). The formulation aims to reduce load shedding, active and reactive power loss, and network voltage fluctuations during DG outages.

Keyword terms: Plug-in Electric Vehicle, hybrid energy storage system, super capacitor, energy allocation.

I. INTRODUCTION

Distributed generators (DGs) can transform conventional power distribution systems into active networks [1]. DGs offer technical, economic, and environmental benefits to utilities and customers (in case of renewables).

DGs reduce power loss, regulate voltage, improve system reliability and loadability, improve power quality, relieve transmission and distribution networks, and increase energy efficiency [2]. DGs save fuel, transmission and distribution costs, and wholesale electricity prices. Optimal siting and sizing of DG units are major steps for DG benefits. Microgrids can be used as a resiliency resource to improve the power system [3–10]. Planning for system resiliency may improve future smart microgrids' resiliency.

Researchers apply different approaches to optimize the optimal siting and sizing of DGs. Minimize power loss [1-3, 10–16], improve voltage profile, improve system stability [15-17], improve loading margin [18], maximize profit, and reduce harmful emissions [18–20]. Different researchers have used single- and multi-objective functions to place DGs optimally. Analytical approaches [1-3], mixed-integer non-linear programming [15], particle swarm optimisation [12-17], genetic algorithms [15], sensitivity analysis [11], and hybrid probabilistic load models to sit and size DGs and used vulnerable node identification to place DGs.

Microgrids are popular in medium- and low-voltage distribution systems because they can support DG penetration. Multi-microgrid networking is an advanced form of the single-microgrid concept. Recent studies have examined transforming radial distribution networks into autonomous networked microgrids. Due to networked microgrids' autonomous operation, system resiliency is needed to handle major disturbances. Resiliency is the power system's ability to withstand high-impact, low-probability events without disrupting critical loads. Researchers consider optimal microgrid sizing strategies and solved a microgrid's multi-objective sizing problem using GA and PSO to size DGs in an islanded microgrid considering total capital, operational, maintenance, and replacement costs and evolution to size DGs in microgrids. GA and its variants have been used to size microgrid components for remote community electrification [20]. DG siting and sizing are focused on improving voltage profile and/or minimizing loss in distribution networks, according to the literature. Recently, [18-20] considered DG siting and sizing for autonomous microgrid networks. Autonomous operation is discussed in [21]. These studies don't consider the microgrids' resiliency. This can disrupt autonomous microgrids during DG outages. Disruptions can cause microgrid residents discomfort and financial loss. Autonomous microgrids must be resilient to reliably serve their critical loads. This paper attempts to improve smart microgrid resiliency by planning for DG outages in autonomous networked microgrids. Initially, N DGs

were placed in a conventional distribution network to create networked microgrids. Then, optimal DG sizing and siting was done by considering 1 to N-1 DG outages from the previous step. This paper uses PSO and GA because they are widely used for siting and sizing DGs. A resilient autonomous microgrid network can provide electricity to consumers during major disturbances, in test balanced distributions are considered (IEEE 33-bus and IEEE 69-bus). This paper's contributions are:

- PSO and GWO transform conventional distribution systems into autonomous microgrids.
- Siting and sizing additional N DGs in the transformed autonomous microgrid network creates a resilient network that can guarantee service reliability even if N-1 DGs are disrupted.
- Finally, microgrid clusters are formed to operate autonomously in normal mode and support each other during DG outages.

This paper continues as follows. Section 2 discusses the transformation of conventional power systems. Section 3 explains the proposed resiliency enhancement scheme, followed by Section 4. Section 5 presents 33- and 69-bus simulation results. Section 6 presents results discussion and analysis, followed by conclusions.

II. DG placement and Islanded microgrid networks

To improve service reliability, conventional distribution networks are converted into microgrids. The switches can connect or disconnect microgrids and help them withstand major disturbances. For transforming a conventional radial distribution system to an autonomous microgrid network, optimal sizing and siting of DGs are required to minimise power loss, regulate voltage deviations in each bus within specified limits, and enhance the network's resiliency to minimise load shedding during major disruption events.

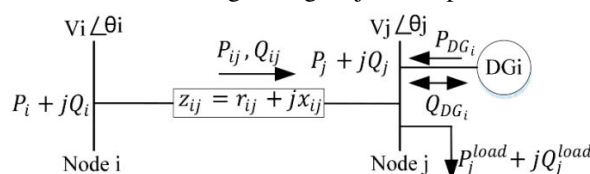


Fig. 1 One line diagram of a simple distribution network with two nodes

Minimizing power loss

Different researchers have considered placing DGs to reduce active and reactive power losses. This paper considers total loss (active and reactive) when siting and sizing DGs. Eq 1 and 2 are exact loss formulas for calculating the system's real and reactive power losses, respectively. Fig. 1 shows a single-line diagram of two nodes i and j).

$$P_L = \sum_{i=1}^n \sum_{j=1}^n (\alpha_{ij} (P_i P_j + Q_i Q_j) + \beta_{ij} (Q_i P_j - P_i Q_j))$$

$$Q_L = \sum_{i=1}^n \sum_{j=1}^n (\gamma_{ij} (P_i P_j + Q_i Q_j) + \delta_{ij} (Q_i P_j - P_i Q_j))$$

where

$$P_i = P_{DG_i} - P_i^{load}, \quad Q_i = Q_{DG_i} - Q_i^{load}$$

$$\alpha_{ij} = \frac{r_{ij}}{V_i V_j} \cos(\theta_i - \theta_j), \quad \beta_{ij} = \frac{r_{ij}}{V_i V_j} \sin(\theta_i - \theta_j)$$

$$\gamma_{ij} = \frac{x_{ij}}{V_i V_j} \cos(\theta_i - \theta_j), \quad \delta_{ij} = \frac{x_{ij}}{V_i V_j} \sin(\theta_i - \theta_j)$$

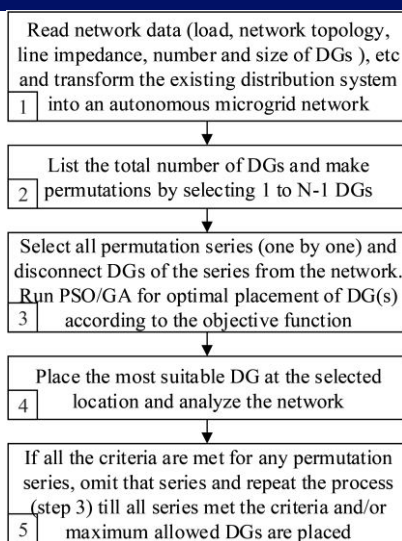


Fig. 2 Algorithm for placing DGs to improve the resiliency of islanded microgrids

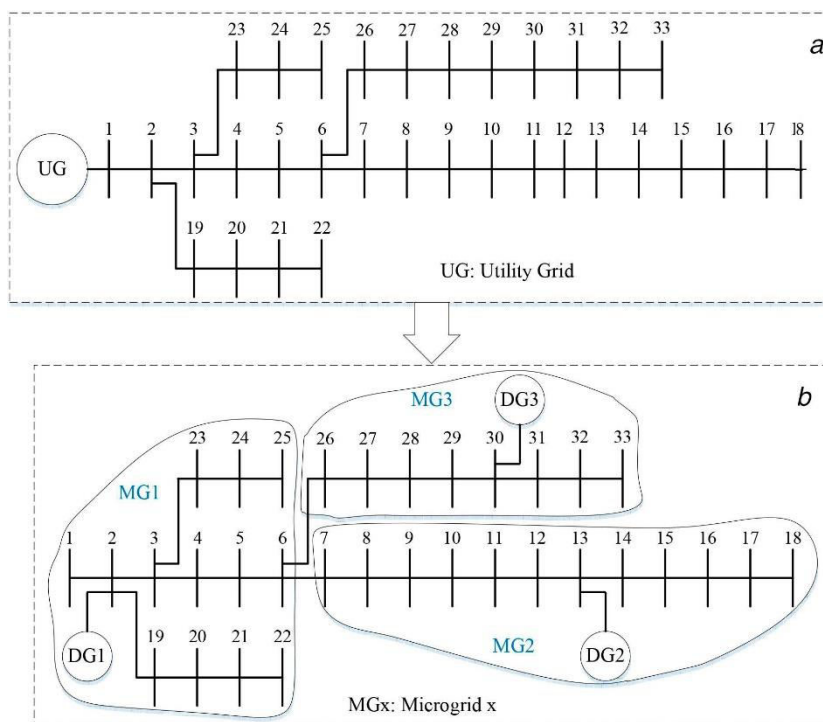


Fig. 3 Clustering of existing distribution system to networked islanded microgrids

III. RESULTS AND DISCUSSION

A. Algorithm for reliability assessment of microrid based distribution system

Maximum DGs per bus are limited by Due to resilience-oriented sizing, each bus can only carry one DG. Initial network transformation has a limited number of DGs, N . Similarly, the number of permissible DGs (N') for transitioning an autonomous network to a resilient network is given, where u_i represents an initial DG at bus i and u_i' indicates an additional DG at bus i .

Before adopting the proposed strategy, the maximum number of DGs for network transformation and resiliency augmentation must be determined. DG types must also be chosen. Intermittent renewable DGs would require batteries. Policymakers must choose these characteristics to balance cost and resilience.

As a minimization objective function, the best position for the lowest objective function value for each particle is supplied, and the global best position among all particles can be expressed. Each iteration updates each particle's position and velocity. Random initial velocities and locations are updated. This study uses 2 for c_1 and c_2 . Particle weights are 0.4 (minimum) and 0.9 (maximum). Transformation and resiliency use the same criteria.

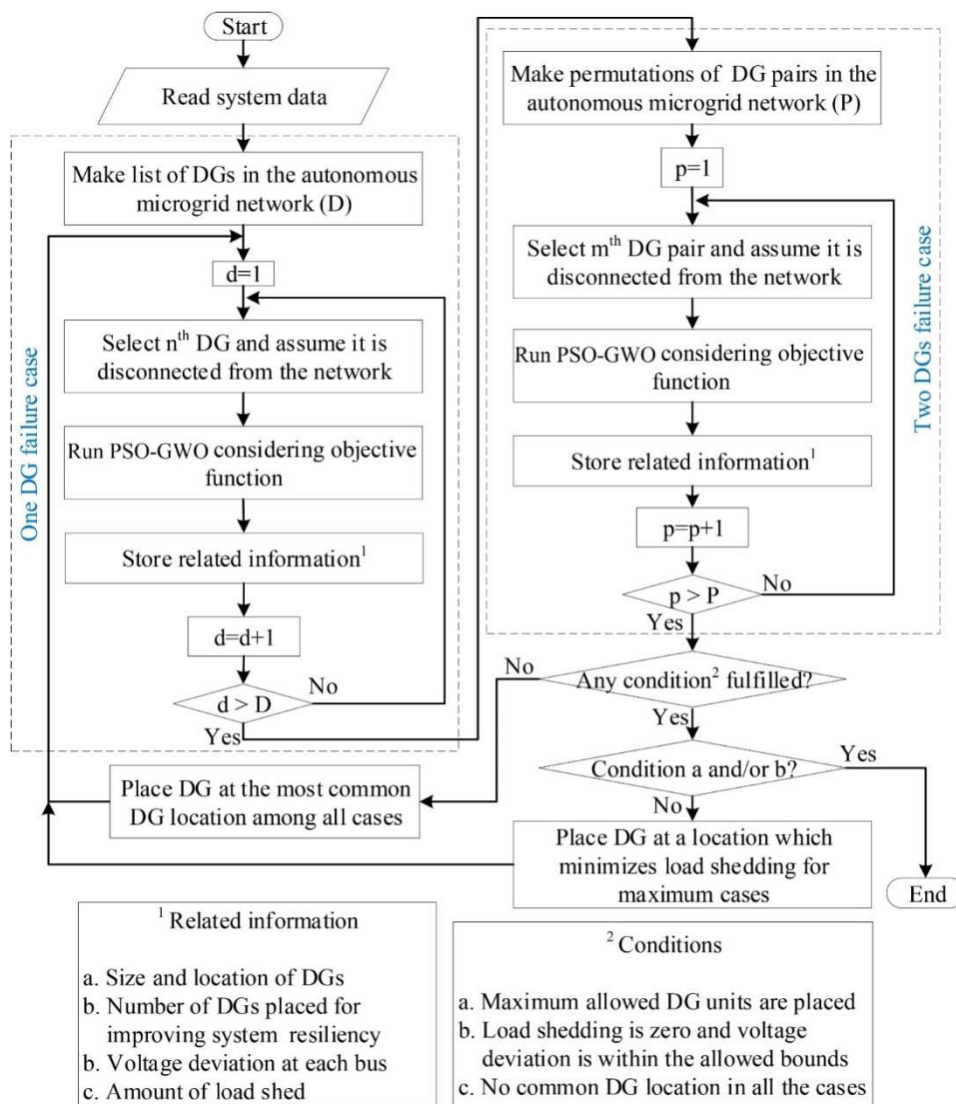


Figure 3 Flowchart for enhancing resiliency of transformed network

Maximum DGs per bus are limited by Due to resilience-oriented sizing, each bus can only carry one DG. Initial network transformation has a limited number of DGs, N . Similarly, the number of permissible DGs (N') for transitioning an autonomous network to a resilient network is given, where u_i represents an initial DG at bus i and u_i' indicates an additional DG at bus i . Before adopting the proposed strategy, the maximum number of DGs for network transformation and resiliency augmentation must be determined. DG types must also be chosen. Intermittent renewable DGs would require batteries. Policymakers must choose these characteristics to balance cost and resilience. As a minimization objective function, the best position for the lowest objective

function value for each particle is supplied, and the global best position among all particles can be expressed. Each iteration updates each particle's position and velocity. Random initial velocities and locations are updated. This study uses 2 for c_1 and c_2 . Particle weights are 0.4 (minimum) and 0.9 (maximum). Transformation and resiliency use the same criteria. GWO is extensively used for sizing and locating DGs alongside PSO due to its easily dispersed, parallel, and survival of the fittest strategy. GWO's features allow for faster optimization. Flow chart showing how GWO determines best location(s) for DG units in distribution system.

B. Illustrated examples

The standard IEEE 33-bus and IEEE 69-bus distribution systems are considered for evaluating the effectiveness of the proposed method. PSO and GWO are used for both sizing and siting of DGs in all the cases. In the case of PSO, total 100 particles and maximum 100 iterations are used, whereas in case of GWO 100 prey agents with a population size of 50 chromosomes are used for the simulations. The acceptable bound for voltage deviation is taken as ± 0.5 pu. The base value for complex power is 10 MVA and voltage is 22.9 kV. The step-by-step process of both 33- and 69-bus systems is explained in the following sections.

Case A: IEEE 33-bus Distribution system with Microgrids

Network transformation

First, the program converts the normal distribution system into a microgrid. Minimizing the goal function determines the size and location of three [36]-like DGs. Table 5.1 lists the active and reactive powers and bus numbers of the three DGs chosen by PSO and GWO. By establishing three DGs, the typical IEEE 33-bus system can be turned into three microgrids (Fig. 5.11). Fig. 5.12 shows the 33bus voltage profiles before and after DG placement. Fig. 5.12 shows that putting DGs with PSO and GWO improves voltage profile. PSO and GWO suggest DG positions to determine voltage deviation. Fig. 5.12 shows that all buses have acceptable voltage variations. Load shedding is determined by deploying the three DGs at PSO and GWO-specified sites. After installing the three DGs, load shedding has decreased to zero, indicating an autonomous microgrid network.

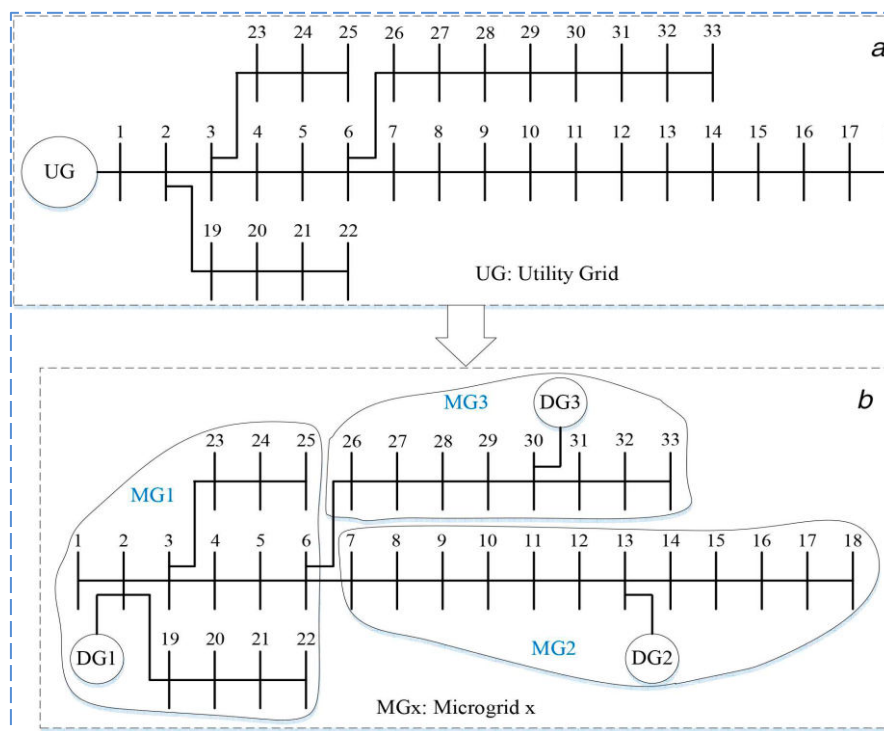


Figure 4 Transformation of IEEE 33-bus distribution system to networked microgrids

DG selection

After transitioning the conventional network into an autonomous microgrid network, the second stage is to evaluate the network's robustness and place DGs to enhance its resiliency. The proposed technique considers 1 to N 1 DG outages. Since three DGs are in the previous step, single and pair failures are examined here. DG2, DG13, and DG30 are single DG outages, and DG2 and DG13, DG13 and DG30, and DG2 and DG30 are DG-pair failures. Fig. 5.2 shows how all six examples are tested and saved.

The most-repeated DG site is chosen after one round. If load shedding occurs, the DG with the highest active power is chosen, otherwise the DG with the lowest active power. Each round, heuristic algorithms suggest a restricted amount of DGs. Maximum DGs for IEEE 33-bus system are 3, 2, 1, and 1. Depending on the frequency of occurrences and other rules, one DG (from those recommended by heuristic algorithms) is chosen in each round.

Table 1 lists reoccurring DGs for PSO and GWO along with their sizes. The remaining section will explain the PSO algorithm's workings simply. GWO results are tabulated with PSO results. Bus 1 is chosen after analyzing the most frequent location (five occurrences). Due to PSO load shedding, DG is sized at $2+1.44995j$ (maximum active power). All six-outage situations are replicated with the specified DG ($2+1.44995j$) on bus 1. Table 3 lists DGs for PSO and GWO. Bus 24 is the second DG because location 24 is repeated four times. In load shedding, the highest active power DG ($1.0242+0.5680j$) is chosen.

Table 1 Size and location of DGs for network transformation

Bus no.	PSO-based size, MW/MVAr		GWO-based size, MW/MVAr	
	Active power	Reactive power	Active power	Reactive power
2	1.8476	2.0000	1.9947	0.9297
13	0.8389	0.3875	0.8137	0.4908
30	1.0833	1.0223	1.0890	0.0375

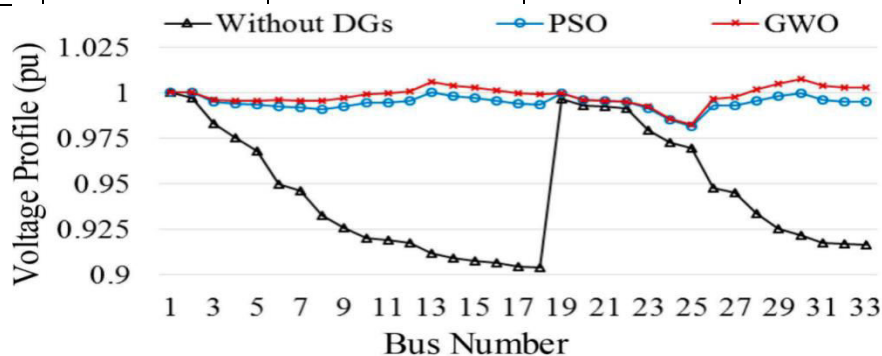


Figure voltage profile at 33 buses

The second DG ($1.0242+0.5680j$) is placed on bus 24 after the second round. Third DG ($1.0142+0.9809j$) is placed on bus 29 after analyzing third-round data (Table 5.14). Due to no load shedding, the lowest active power DG is chosen. After installing the third DG, all six outages have ended. DG 13 and 30 failures exceed voltage limit deviations. This case gets an extra DG. PSO calculates $0.2+0.0j$ at bus 16 and GWO $0.06+0.34j$. 5.1.4 discusses voltage variations.

Load shedding

Literature discusses major power system events' frequency and intensity. These big disturbances might cause DG outages. These disruptions may produce load shedding and comfort customers, especially in autonomous microgrid networks. The resiliency of the converted microgrid network is analyzed, and DGs are deployed to minimize load shedding.

The converted network considers single DG and DG pair outages and determines load shedding using PSO and GWO. Table 5 shows that none of the six DG scenarios require load shedding. By placing the first DG on bus 1, load shedding is eliminated for single DG failures. Table 5.5 shows that DG-pair failures still cause load shedding.

Second DG is placed on bus 24, however load-shedding continues during DG2 and DG30 outages. A third DG is placed on bus 29 according to placement and size requirements. Table 5.5 shows that installing the third DG on bus 29 eliminated load shedding for DG-pair failure. Fourth DG is placed to avoid voltage bound violations (1 0.5 pu). DG pair 13 and 30 outages occur after inserting DG 3. Voltage violation is avoided by placing the fourth DG on bus 16. The next part discusses the voltage limits of all six outage instances after each round.

Voltage regulation

Fig. 5.7 depicts the network bus voltage patterns for each single DG outage condition. Fig. 5.8 illustrates the network bus voltage trends after each round for all three DG-pair outages. Fig.5.7 shows that after placing one DG at position 1, the voltage profile of DG 2 outage case is acceptable (after the first round). Third-round voltage profiles for DG 13 and DG 30 outages are allowed (placing DGs at 1, 24, and 29 buses). After the third round (installing DGs at 1, 24, and 29 buses), voltage profiles for two DG-pair outage instances, DGs 2 and 13 and DGs 2 and 30, are acceptable. Third DG pair failure (DGs 13 and 30) voltage profile violates buses 13–18. The fourth DG must be installed to bring buses 13–18's voltage profiles within range. After putting the fourth DG at bus 16, as determined by PSO, the voltage profile for the third DG-pair outage case improved. All 33 buses' voltage profiles during six probable outages are now acceptable. Table 5.6 shows that load shedding is eliminated in all circumstances.

GWO suggests adding four DGs to the IEEE 33-bus distribution system, like PSO. Fig. 5.9 shows the network voltage curve after DG placement (per GWO). Fig. 5.9a illustrates the voltage profile for a single DG failure, while Fig. 5.9b depicts DG-pair outages. All six voltage profiles are allowed. Table 5.5 shows that load shedding has also been eliminated.

Total power loss

After inserting DGs according to Section 5.4.1.2, the overall network power loss (active and reactive) is monitored for all six probable outages. If load shedding is zero and no buses break voltage limitations during an outage, overall power loss for that scenario is excluded for the next round. Due to comparable patterns, only PSO is explained here.

Fig. 5.10 depicts network power loss for single DG outages. After the first round, Fig. 5.10 does not show total loss for DG2 outage. Table 5.5 and Fig. 5.7a show that after deploying a DG on bus 1, there is no load shedding and voltage profile deviations are acceptable. Total power loss for single DG outages is also not shown during the fourth round. Total power loss has decreased after DG and PSO deployment, as shown in Fig. 5.10.

Table 3 Load shedding in the autonomous microgrid network [MW]

Method	DG failure		Load Shedding in MW				
			No DG	1	1 and 24	1, 24 and 29	1, 24, 29, and 16
PSO	Single DG	2	1.9669	0.0000	0.0000	0.0000	0.0000
		13	0.8584	0.0000	0.0000	0.0000	0.0000
		30	1.1339	0.0000	0.0000	0.0000	0.0000
	DG pair	2,13	2.9567	0.7117	0.0000	0.0000	0.0000
		13,30	2.0648	0.0706	0.0000	0.0000	0.0000
		2,30	3.9120	0.9895	0.0143	0.0000	0.0000
GWO	Single DG	2	1.9859	0.0000	0.0000	0.0000	0.0000
		13	0.7053	0.0000	0.0000	0.0000	0.0000

		30	0.0120	0.0000	0.0000	0.0000	0.0000
	DG pair	2,13	2.9507	0.7117	0.0000	0.0000	0.0000
		13,30	1.9177	0.0706	0.0000	0.0000	0.0000
		2,30	3.9372	0.9895	0.0000	0.0000	0.0000

Fig. 5.11 demonstrates network power loss during DG-pair outages. After the third round (installing DGs on buses 1, 24, and 29), load shedding has been eliminated for all three DG-pair failure instances. DGs 2 and 13 and DGs 2 and 30 outage voltage deviations are likewise within limits. In round 4, only DGs 13 and 30 outage cases exhibit total power loss. Fig. 5.11 shows that overall power loss has decreased after DG installation and PSO convergence.

Resilient autonomous microgrid network

The resilient autonomous microgrid network built by four DGs in Fig. 5.3b. Fig. 5.12 shows the finished PSO and GWO resilient microgrid networks. Four additional DGs formed six autonomous microgrids (Fig. 5.12). All microgrids can operate independently while tie switches are open. In emergencies, tie switches can transmit electricity between electrically connected microgrids. The resilient autonomous microgrid network can handle single and double DG failures.

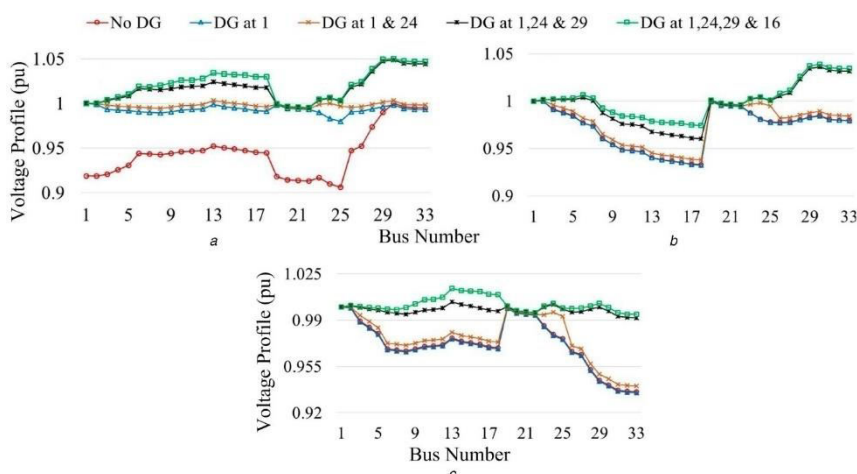


Figure Voltage profiles of network buses for single DG outage cases (a) DG 2, (b) DG 13, (c) DG 30

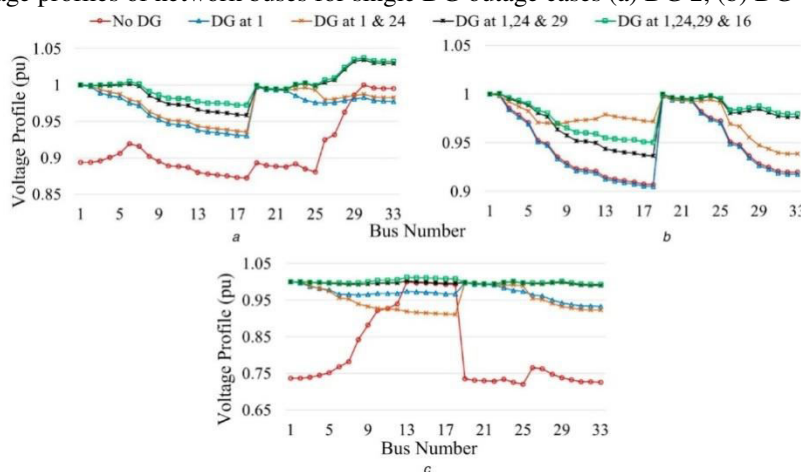


Fig Voltage profiles of network buses for DG-pair outage cases (a) DGs 2 and 13, (b) DGs 13 and 30, (c) DGs 2 and 30

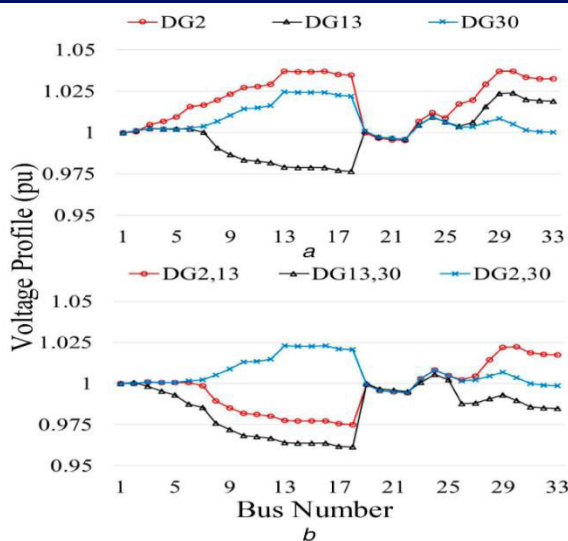


Fig. Voltage profiles of network buses for DG outage cases (a) Single DG outage, (b) DG-pair outage

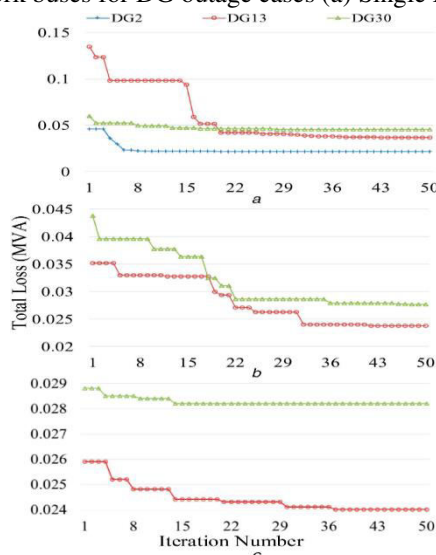


Fig. Total network losses for single DG outage cases (a) Round 1, (b) Round 2, (c) Round 3

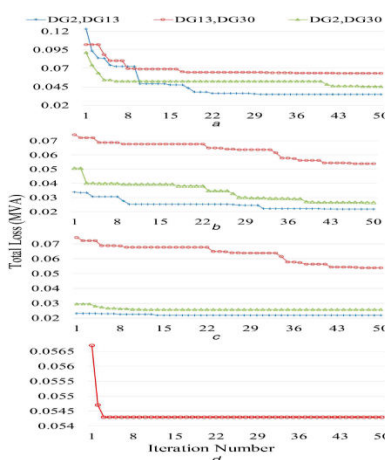


Fig. Total network losses for DG-pair outage cases (a) Round 1, (b) Round 2, (c) Round 3, (d) Round 4

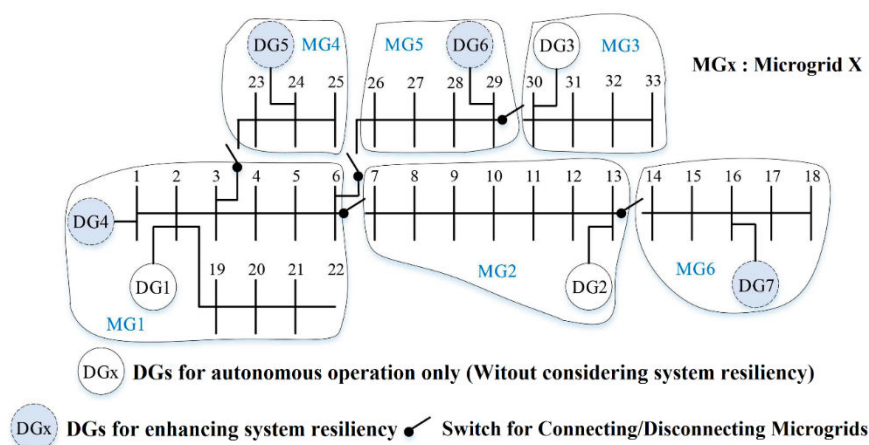


Figure Transformed IEEE 33-bus resilient autonomous network with microgrids

Case B: IEEE 69-bus Distribution system with Microgrids

Network transformation

First, the program converts the normal distribution system into a microgrid. Like the 33-bus system, the 69-bus system becomes a microgrid network. Minimizing objective function determines the size and location of three DGs. Similar to the 69-bus scheme, three DGs are evaluated. Same procedure can be used for more than three DGs. Table 5.8 lists the size and position of PSO and GWO's three DGs. The typical IEEE 69-bus system (Fig. 5.15a) can be turned into three microgrids (Fig. 5.15b) by adding three DGs. Fig. 5.16 shows the voltage profiles of all 69 buses before and after DGs. Voltage variations are within the permissible range for all buses after placing DGs at PSO and GWO-suggested positions. Load shedding is determined by deploying the three DGs at PSO and GWO-specified sites. After installing the three DGs, load shedding has decreased to zero, indicating an autonomous microgrid network.

DG selection

Consider the outage of 1 to N 1 previously placed DGs to evaluate the network's resilience. Since three DGs are put in the previous step, this step considers a single DG and DG pair failure. DG1, DG60, and DG69 are single DG outages, and DG1 and DG60, DG1 and DG69, and DG60 and DG69 are DG-pair failures. The most-repeated DG site is chosen after one round. DG size rules are the same as for 33-bus systems. Table 5.7 lists repeated DGs for PSO and GA and their sizes. The remaining section will explain the PSO algorithm's workings simply. GWO results are tabulated with PSO results. The first bus 49 DG is $0.5486 + 0.4339j$ for PSO. Table 5.8 lists second-round DG occurrences for PSO and GWO. Bus 2 has a $2 + 2j$ second DG. Analyzing third-round data (Table 5.9).

Table 5.6 Size and location of DGs for network transformation

Bus no.	PSO-based size, MW/MVAr		GWO-based size, MW/MVAr	
	Active power	Reactive power	Active power	Reactive power
1	5	0.0025	3.5000	0.8700
60	1.2381	1.2390	1.0628	1.0412
69	0.5519	0.3721	1.0819	1.7516

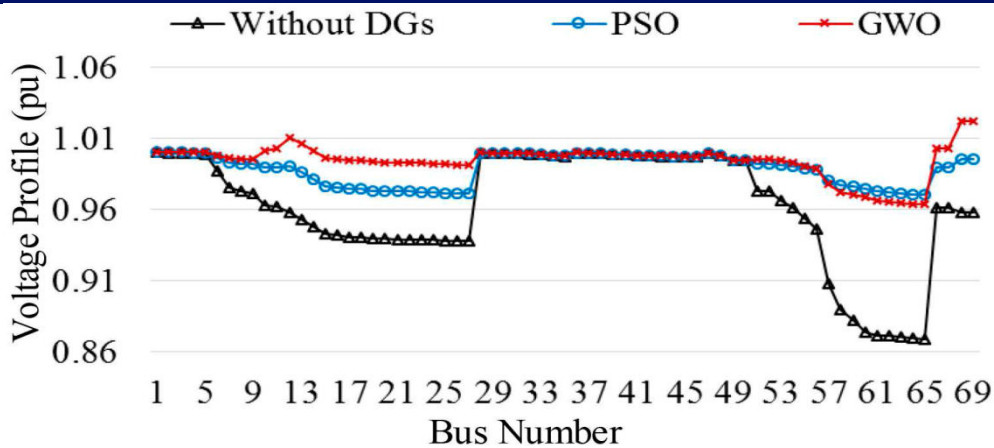


Figure 5.14 Voltage profiles of original and transformed networks

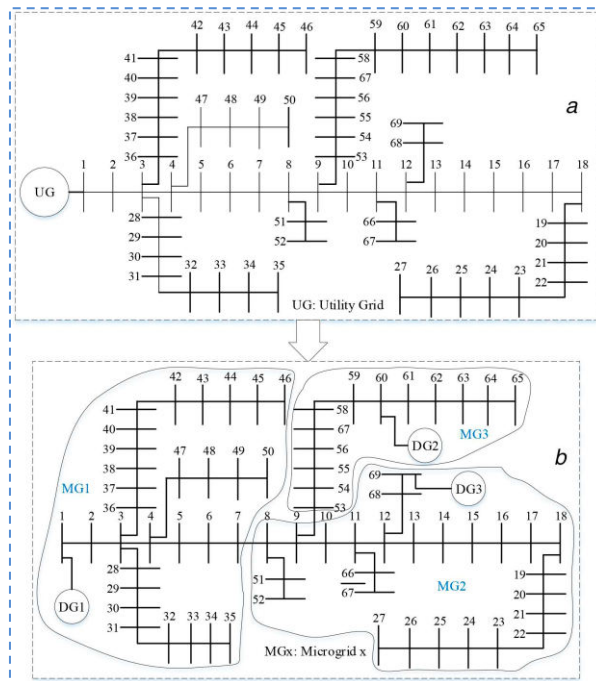


Figure Transformation of IEEE 69-bus distribution system to networked microgrids

Load shedding

The converted network considers single DG and DG pair outages and determines load shedding using PSO and GWO. Table 5.10 shows that load shedding occurs almost always for no DG. Load shedding is eliminated in all six scenarios by adding three DGs.

Voltage regulation

PSO and GWO advise adding three DGs to the IEEE 69-bus system. Fig. 15 shows the network voltage profile after PSO DG placement, and Fig. 16 shows GWO. Figs. 15a and 16a show the voltage profile for a single DG outage, while Figs. All six voltage profiles are allowed.

Total power loss

After inserting DGs according to Section 5.4.1.2, the overall network power loss (active and reactive) is monitored for all six probable outages. If load shedding is zero and no buses break voltage limitations during an outage, overall power loss for that scenario is excluded for the next round. Due to comparable patterns, only PSO is explained here. Fig. 5.10 depicts network power loss for single DG outages. After the first round, Fig. 5.10 does not show total loss for DG2 outage. Table 5.5 and Fig. 5.7a show that after deploying a DG on bus 1, there is no load shedding and voltage profile deviations are acceptable. Total power loss for single DG outages is also not shown during the fourth round. Total power loss has decreased after DG and PSO deployment, as shown in Fig. 5.10.

Fig. 5.11 demonstrates network power loss during DG-pair outages. After the third round (installing DGs on buses 1, 24, and 29), load shedding has been eliminated for all three DG-pair failure instances. DGs 2 and 13 and DGs 2 and 30 outage voltage deviations are likewise within limits. In round 4, only DGs 13 and 30 outage cases exhibit total power loss. Fig. 5.11 shows that overall power loss has decreased after DG installation and PSO convergence.

Resilient autonomous microgrid network

The resilient autonomous microgrid network built by three DGs in Fig. 13b. Figure 17 shows the final resilient microgrid network for PSO and GWO. Three additional DGs form five autonomous microgrids. The resilient autonomous microgrid network can handle single and double DG failures.

Table 5.14 Load shedding in the autonomous microgrid network [MW]

Method	DG failure		Load Shedding in MW			
			No DG	49	49 and 2	49, 2 and 59
PSO	Single DG	1	2.0119	1.4633	0.0000	0.0000
		60	0.0000	0.0000	0.0000	0.0000
		69	0.0000	0.0000	0.0000	0.0000
	DG pair	1, 60	3.2500	2.7014	0.7014	0.0000
		1, 69	2.5638	2.0152	0.0975	0.0000
		60, 69	0.0000	0.0000	0.0000	0.0000
GWO	Single DG	1	1.6572	0.4452	0.0000	0.0000
		60	0.0000	0.0000	0.0000	0.0000
		69	0.0000	0.0000	0.0000	0.0000
	DG pair	1, 60	2.7200	1.5080	0.0000	0.0000
		1, 69	2.7391	1.5271	0.0000	0.0000
		60, 69	0.3019	0.0000	0.0000	0.0000

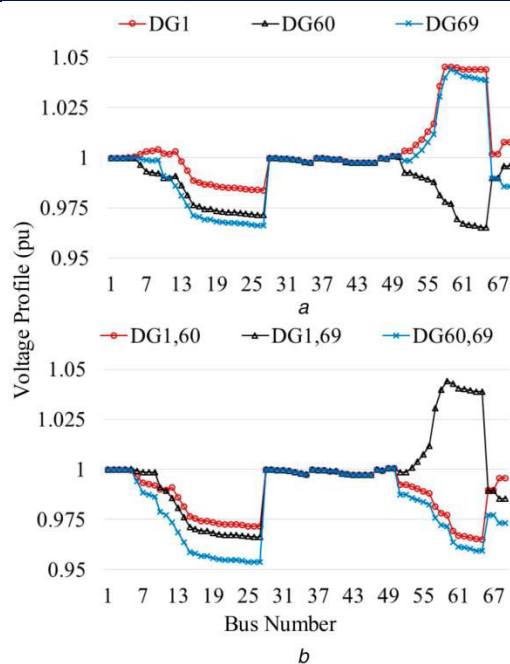


Figure Voltage profiles of network buses for DG outage cases (a) Single DG outage, (b) DG-pair outage

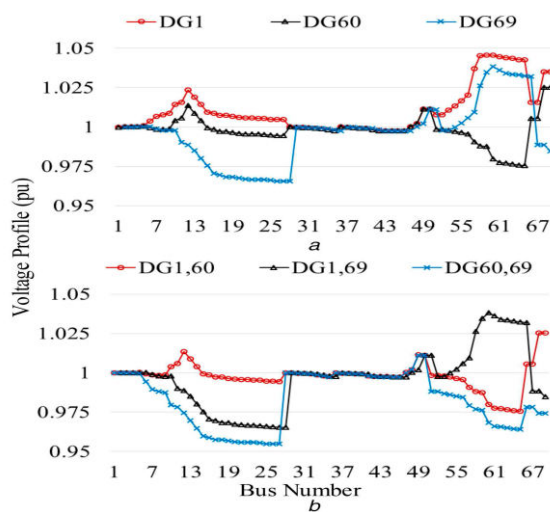


Fig.5.8 Voltage profiles of network buses for DG outage cases (a) Single DG outage, (b) DG-pair outage

Table 5.15 Summary of voltage profile deviations

Bus system	Method	Maximum	Minimum
IEEE 33-bus system	no DG	1.000	0.903
	PSO	1.001	0.982
	GWO	1.008	0.983
IEEE 69-bus system	no DG	1.000	0.869
	PSO	1.000	0.970
	GWO	1.022	0.964

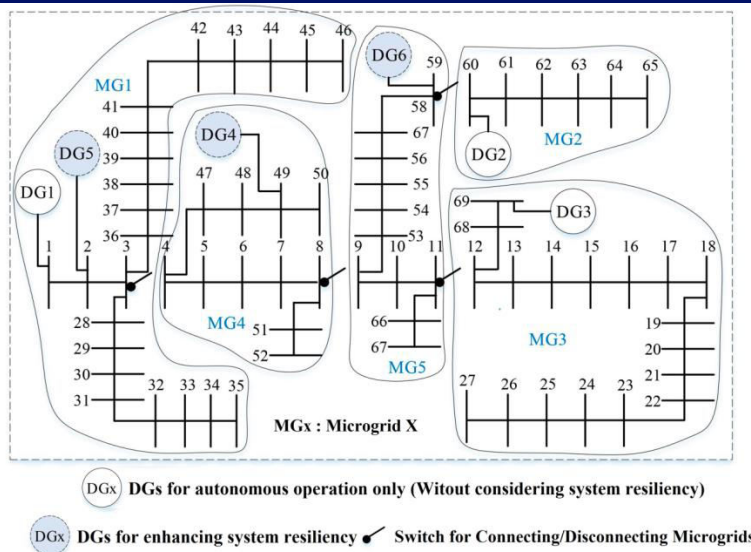


Figure 5.21 Transformed resilient autonomous network of IEEE 69-bus system

Table 5.16 Summary of resiliency-oriented DG sizes

Bus system	Parameter	Unit	PSO	GWO
IEEE 33-bus system	Active power	MW	4.238	4.455
	Reactive power	MVAr	2.998	3.333
	Number of DGs	—	4	4
IEEE 69-bus system	Active power	MW	3.818	4.557
	Reactive power	MVAr	3.690	4.633
	Number of DGs	—	3	3

Table 5.16 Summary of loss reduction via DG placement

Bus system	Method	Loss reduction, %
IEEE 33-bus system	no DG	0.00
	PSO	77.16
	GWO	77.47
IEEE 69-bus system	no DG	0.00
	PSO	90.14
	GWO	90.23

Conclusion:

IEEE 33-bus and IEEE 69-bus distribution networks become three microgrids. Single DG outages and DG pairs are used to evaluate the microgrid's resilience. PSO and GWO discover appropriate DG locations and sizes to reduce load shedding during significant disturbances. After each round, one DG is chosen depending on the number of outage repeats.

Load shedding determines DG size. This method is repeated until all permissible DGs are placed or voltage violation and load shedding are eliminated for all six outage scenarios. Fitness function considers voltage violations, load shedding, and power loss. Finally, additional DGs are placed to establish a resilient network of microgrids. A network planner can use the proposed method to create robust microgrid networks. By powering loads during DG outages, the suggested technique can improve consumer comfort and reduce financial loss. Tie switches can be used to connect autonomous microgrid pairs during disturbances. The proposed technique can guarantee service reliability even if two of the three main DGs (installed initially for network transformation) are disrupted.

References:

- [1] R. Uluski, J. Kumar, S. M. Venkata et al., "Microgrid controller design, implementation, and deployment: a journey from conception to implementation at the philadelphia navy yard," *IEEE Power and Energy Magazine*, vol. 15, no. 4, pp. 50–62, 2017.
- [2] H. Laaksonen, D. Ishchenko, and A. Oudalov, "Adaptive protection and microgrid control design for hailuoto island," *IEEE Transactions on Smart Grid*, vol. 5, no. 3, pp. 1486–1493, 2014.
- [3] R. H. Lasseter and D. Smart, "Smart distribution: coupled microgrids," *Proceedings of the IEEE*, vol. 99, no. 6, pp. 1074–1082, 2011.
- [4] T. Ding, Y. Lin, Z. Bie, and C. Chen, "A resilient MicroGrid Formation strategy for load restoration considering masterslave distributed generators and topology reconfiguration," *Applied Energy*, vol. 199, pp. 205–216, 2017.
- [5] M. V. Kirthiga, S. A. Daniel, and S. Gurunathan, "A methodology for transforming an existing distribution network into a sustainable autonomous micro-grid," *IEEE Transactions on Sustainable Energy*, vol. 4, no. 1, pp. 31–41, 2013.
- [6] X. Wei, X. Xiangning, and C. Pengwei, "Overview of key microgrid technologies," *International Transactions on Electrical Energy Systems*, vol. 28, no. 7, p. e2566, 2018.
- [7] T. Rawat, K. R. Niazi, N. Gupta, and S. Sharma, "Impact analysis of demand response on optimal allocation of wind and solar based distributed generations in distribution system," *Energy Sources, Part B: Economics, Planning and Policy*, vol. 16, no. 1, pp. 75–90, 2021.
- [8] M. A. Tolba, A. A. Zaki Diab, V. N. Tulsy, and A. Y. Abdelaziz, "Vlci approach for optimal capacitors allocation in distribution networks based on hybrid psogsa optimization algorithm," *Neural Computing & Applications*, vol. 31, no. 8, pp. 3833–3850, 2019.
- [9] M. Pesaran Ha, P. D. Huy, and V. K. Ramachandaramurthy, "A review of the optimal allocation of distributed generation: objectives, constraints, methods, and algorithms," *Renewable and Sustainable Energy Reviews*, vol. 75, pp. 293–312, 2017.
- [10] R. Sanjay, T. Jayabarathi, T. Raghunathan, V. Ramesh, and N. Mithulananthan, "Optimal allocation of distributed generation using hybrid grey wolf optimizer," *IEEE Access*, vol. 5, pp. 14807–14818, 2017.
- [11] B. Poornazaryan, P. Karimyan, G. B. Gharehpetian, and M. Abedi, "Optimal allocation and sizing of dg units considering voltage stability, losses and load variations," *International Journal of Electrical Power & Energy Systems*, vol. 79, pp. 42–52, 2016.
- [12] Q. Zhao, S. Wang, K. Wang, and B. Huang, "Multi-objective optimal allocation of distributed generations under uncertainty based on D-S evidence theory and affine arithmetic," *International Journal of Electrical Power & Energy Systems*, vol. 112, pp. 70–82, 2019.
- [13] M. Farzinfar, M. Shafiee, M. Amirahmadi, and A. Kia, "Determination of optimal allocation and penetration level of distributed energy Resources considering short circuit currents," *International Journal of Engineering*, vol. 33, no. 3, pp. 427–438, 2020.
- [14] P. del Rio, A. Papadopoulou, and N. Calvet, "Dispatchable res and flexibility in high res penetration scenarios: solutions for further deployment," *Energy Sources, Part B: Economics, Planning and Policy*, vol. 16, no. 1, pp. 1–3, 2021.



International Journal for Innovative Engineering and Management Research

PEER REVIEWED OPEN ACCESS INTERNATIONAL JOURNAL

www.ijemr.org

[15] M. Saric, J. Hivziefendic, T. Konjic, and A. Ktena, "Distributed generation allocation considering uncertainties," *International Transactions on Electrical Energy Systems*, vol. 28, no. 9, Article ID e2585, 2018.